Process of image Super-Resolution

Sébastien LABLANCHE[1,*], Gérard LABLANCHE[2,†],

1 Université Paul Sabatier Toulouse III, Route de Narbonne, 31330 Toulouse
2 Université de Bordeaux, 351 Cours de la Libération, 33400 Talence

†Email: gerard.lablanche@orange.fr

Abstract

In this paper we explain a process of super-resolution reconstruction allowing to increase the resolution of an image.The need for high-resolution digital images exists in diverse domains, for example the medical and spatial domains. The obtaining of high-resolution digital images can be made at the time of the shooting, but it is often synonymic of important costs because of the necessary material to avoid such costs, it is known how to use methods of super-resolution reconstruction, consisting from one or several low resolution images to obtain a high-resolution image. The American patent US 9208537 describes such an algorithm. A zone of one low-resolution image is isolated and categorized according to the information contained in pixels forming the borders of the zone. The category of it zone determines the type of interpolation used to add pixels in aforementioned zone, to increase the neatness of the images. It is also known how to reconstruct a low-resolution image there high-resolution image by using a model of super-resolution reconstruction whose learning is based on networks of neurons and on image or a picture library. The demand of Chinese patent CN 107563965 and the scientist publication "Pixel Recursive Super Resolution", R. Dahl, M. Norouzi, J. Shlens propose such methods. The aim of this paper is to demonstrate that it is possible to reconstruct coherent human faces from very degraded pixelated images with a very fast algorithm, more faster than compressed sensing (CS) algorithm, easier to compute and without deep learning, so without important information technology resources, i.e. a large database of thousands training images (see `https://arxiv.org/pdf/2003.13063.pdf`). This technological breakthrough has been patented in 2018 with the demand of French patent FR 1855485 (`https://patents.google.com/patent/FR3082980A1`, see the HAL reference `https://hal.archives-ouvertes.fr/hal-01875898v1`).

1.Introduction

Last February 2017, three researchers described before from Google Brain published their results on Pixel Recursive Super Resolution to present the

*Corresponding author: For further information on this publication, please contact Mr Sébastien LABLANCHE, Adress: 21, allée des camélias 33127 Martignas sur jalle, France, Email: gerard.lablanche@orange.fr, Phone: (+33) 0556214179 or (+33) 0647665706.

powerful IA (https://arxiv.org/pdf/1702.00783.pdf). Their technology consists in approaching the final picture by combining an algorithm and database pictures of Google to obtain from an initial 8x8 definition picture, a 32x32 definition picture which is very similar as the actual picture. A French startup named LABLANCHE (http://www.lablanche-and-co.com) is said to have developed an innovation based on a powerful algorithm which could deliver similar results as Google, but, without using any database. If the achievements of this new algorithm are confirmed, it would represent a very important innovation for any potential end user which would want to operate independently of Google database, and faster. In this paper, we present the new technical of interpolation for image super-resolution based on conditional interpolations in three directions called successively to achieve a blurred high resolution image with a lot of more details to help deconvolution algorithm (the directional interpolation monitored by the orientation of the motion filter) to create truth details at the end (LABLANCHE process).

2.Problem

2.1 Presentation

For the tests, we must realize two stages. For the stage 1, we do a compression of images which consists to fill in each bloc of 4x4 pixels of R, G or B channel with an averaging intensity of the bloc. For the stage 2, we do a storage of intensities in a vector of unsigned char type for the channel (if monochrome image) or three channels (if RGB image). In the C++ language, the unsigned char type elements corresponds to bytes. This stage provides a smaller size file which contains averaging intensities. The parameter named step corresponds to the size of same color blocs, step controls the quality of the reconstruction and therefore the loss of quality generated by the compression. For step=4, the compression rate is equivalent of the JPEG size format (step and step/2 must be even numbers to realize the reconstruction). We note q=step/2, the number of levels. Here we have two levels LEVEL 1 and LEVEL 2 and step is an even number which enables to share the 4 by 4 pixels bloc in 4 blocs qxq. In the case of 2 by 2 pixels blocs, we have one level (step=2).

2.2 Modelling

Considering that images as vectors, the problem can be modeled with a low resolution observation named $\mathcal{B}$ of the original image $\mathcal{I}$ which is obtained in applying an operator of movement $\mathcal{M}$ (i.e. a geometric transformation), a blur operator $\mathcal{F}$, and with a subsampling operator $\mathcal{S}$. An additive noise ϵ completes this inverse problem: $\mathcal{B}=\mathcal{SFMI}+\epsilon$. The operator $\mathcal{SFM}$ (subsampling + blurring + geometric transformation) owns more columns that rows, the system is underdetermined. The extension factor between the image $\mathcal{B}$ and the image $\mathcal{I}$ is equal to $step^2$. The image $\mathcal{H}$ obtained by a super-resolution algorithm from $\mathcal{B}$ must be verified the reconstruction constraint, i.e. must gives $\mathcal{B}$ using the observation model.

3.Compressed Sensing

The Compressed Sensing technique makes it possible to find the most parsimonious solution from an undetermined linear system. It involves not only the means of finding such a solution but also the linear systems that are acceptable. The process is to reconstruct accurately a signal or an image when the number of measurements is less than the length of the signal. The paradox can be explained by the fact that the signal admits a sparse representation in an appropriate basis. This sampling aims to replace the classic Shannon sampling. This theory has been widely developed in recent years and the amount of applications is continuing to rise in diverse fields such as tomography with MRI and computed tomography or radar and radar imagery, in particular in signal and image compression. We consider a real valued signal x, which we will see in the form of a column vector of length N. In the case of images or higher dimension signals, we can arrange the data to form a long vector. We indicate this signal in a Ψ base such as x=Ψs. We wish to select the base whereby the majority of coefficients of s are equal to zero, ie x is parsimonious in the Ψ base. These bases are known and usually used to compress the starting signal. Compressed Sensing proposes to acquire directly the compressed version of the signal so that unnecessary samples do not need to be processed. The linear measuring process that is used consists of making M scalar products, with M much smaller than N, between x and a collection of vectors going from 1 to M. We obtain therefore samples $y_j = \langle x, \Phi_j \rangle$ of measurements. Considering that the measurement matrix Φ has the (Φ_j) as column, we can thus write x as: y=Φx=$\Phi\Psi$s=Θs (with Θ=$\Phi\Psi$). The measurement matrix design must be able to find the most parsimonious signals. In order to do so, the measurement matrix must follow certain properties, one of which is called RIP (Restricted Isometry Property). The matrix Φ satisfies the restricted isometry property (RIP) of order k if there exists a δ_k in (0,1) such that $(1\text{-}\delta_k)\|x\|_2^2 \leq \|\Phi x\|_2^2 \leq (1+\delta_k)\|x\|_2^2$ holds for all $x \in \Sigma_k = \{x : \|x\|_0 \leq \mathrm{k}\}$. Furthermore, Φ must be inconsistent with Ψ, so the coherence of the Θ matrix must be closest to 0. The coherence μ of a matrix Θ is the largest absolute inner product between any two columns of Θ and is defined by $\mu(\Theta) = \max\limits_{1 \leq i \leq j \leq n} \frac{\langle \Theta_i, \Theta_j \rangle}{\|\Theta_i\| \|\Theta_j\|}$. It is evident that these properties are satisfied with a high probability simply by choosing Φ at random, for example by using a Gaussian distribution. Although these RIP or inconsistency conditions are satisfactory for some sets of measurements, they are only necessary conditions and not sufficient. There are other properties, also insufficient, which require us to need even less samples in order to guarantee a parsimonious signal reconstruction. The last step of the Compressed Sensing process is the reconstruction of the starting signal. For this, we know the M values for y, the matrix measurements used as well as the Ψ base. The reconstruction algorithm seeks to find the coefficients of s. Thanks to the knowledge of Ψ, it is then simple to find x, the starting signal. There are infinite solutions for the equation Θs=y, however we are looking for the solution which minimises a certain norm. The L2 norm measures the signal energy which is why by using a L2-Minimization, we will hardly ever find a K-parsimonious result. The L0

norm measures the parsimony of the signal (we count the number of elements not equal to zero), the optimization $\hat{s}$=arg min$\|s\|_0$ such as Θs=y gives a good result (L0-Minimization). The disadvantage is that this problem can not be calculated digitally. It has been shown that the optimization based on the L1 norm makes it possible to find an exact K-parsimonious signal, the problem of the L1-Minimization is convex. Its resolution could be reduced to a linear program, more often known as basis pursuit. This resolution is not the only one and there are other techniques which allow for even better results such as Conjugate Gradient Pursuit (CGP) or Stagewise Weak Conjugate Gradient Pursuit (StWCGP). The number of necessary measurements M to have an exact recovery of the K-parsimonious signal is in the same order than 5K.

4.Model

We use a reconstruction of the pixelated image with an algorithm of conditional and directional interpolation. The algorithm owns as scientific base the fact when the pixels ratio is very small the decoherence used in compressed sensing (CS) plays an important role in the quality of reconstruction whereas the parsimony plays an important role when the ratio is more important (over 10%). So the parsimony research is efficient for the problem with step=2 but is inefficient for step=4 and step=3. The algorithm mixes the information in order to approach the reality because the decoherence is controled with following conditional interpolations in three possible directions which enables for the deconvolution (the final step called directional interpolation) to create the details to give an acceptable reconstruction.

4.1 Conditional interpolation

We start with a 4x4 pixels bloc filled in with an averaging intensity (B bloc). The B bloc is divided in four similar neighbors 2x2 blocs : B1, B2, B3 and B4. The B1 bloc (at the top and on the left) always keeps its starting intensity. The B bloc (4x4) owns three 4 by 4 neighbors blocs C, D and E and data interpolation is controled by three parameters p2, p3 and p4:

- the C bloc (on the right)
- the D bloc (at the bottom)
- the E bloc (at the bottom and on the right).
- p2 is the parameter which controls the mean between the B bloc and the C bloc
- p3 is the parameter which controls the mean between the B bloc and the D bloc
- p4 is the parameter which controls the mean between the B bloc and the E bloc.

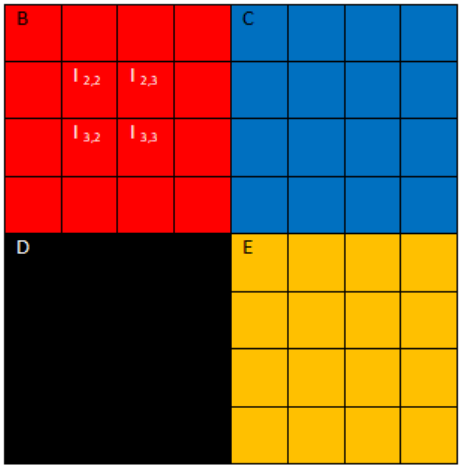

Figure 1: illustration of the image splitting in four neighbor blocs B,C,D,E.

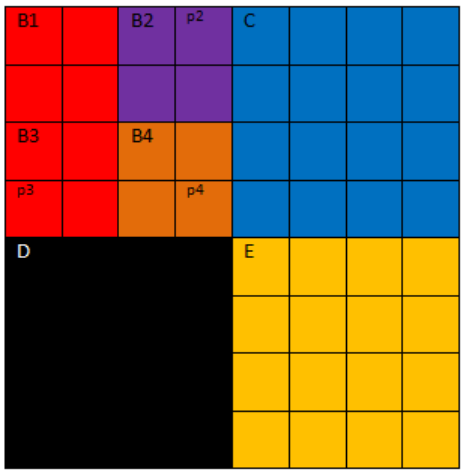

Figure 2: illustration of LEVEL 1 interpolation.

- B1 keeps the color of B bloc (always)
- B2 takes the average color $\frac{(B+C)}{2}$ if $|B-C| \leq p2$ and keeps the B color otherwise
- B3 takes the average color $\frac{(B+D)}{2}$ if $|B-D| \leq p3$ and keeps the B color otherwise
- B4 takes the average color $\frac{(B+E)}{2}$ if $|B-E| \leq p4$ and keeps the B color otherwise.

The setting of p2, p3 and p4 parameters is very important. We realize the interpolation between the two blocs only if they have enough closed colors. These parameters are integers between 0 and 255. If the value is equal to 0, there is no interpolation and if the value is 255, the interpolation is always realized. In other cases, the interpolation is realized if the two adjacent blocs have intensities with a smaller difference than the constraint. The goal of this step is to separate different interest areas of the image and to generate contrast enhancement. We called the LEVEL 1 routine several times with different parameters p2, p3 and p4 to obtain the contrast enhancement and the last call is realized with non conditional interpolations e.g. with p2 = 255, p3 = 255, p4 = 255 in order to have a presmoothing. We use the mean of the central square $\frac{I_{2,2}+I_{2,3}+I_{3,2}+I_{3,3}}{4}$ to colorize the 4 by 4 pixels bloc on Figures 1 and 2. On this example, the B2 bloc and the B4 bloc are changed by interpolation and the B3 bloc keeps its color because of the constraints. We start with the B1 bloc which is divided in 4 neighbours blocs of size 1 (pixels) : B11, B12, B13 and B14, the B11 pixel (at the top and on the left) always keeps the B1 bloc intensity (see Figure 3).

- B11 keeps the color of B1 bloc (always)
- B12 takes the average color $\frac{(B1+B2)}{2}$ if $|B1-B2| \leq p2'$ and keeps the B1 color otherwise
- B13 takes the average color $\frac{(B1+B3)}{2}$ if $|B1-B3| \leq p3'$ and keeps the B1 color otherwise
- B14 takes the average color $\frac{(B1+B4)}{2}$ if $|B1-B4| \leq p4'$ and keeps the B1 color otherwise
- p2' is the parameter which controls the mean between the B1 bloc and the B2 bloc
- p3' is the parameter which controls the mean between the B1 bloc and the B3 bloc
- p4' is the parameter which controls the mean between the B1 bloc and the B4 bloc.

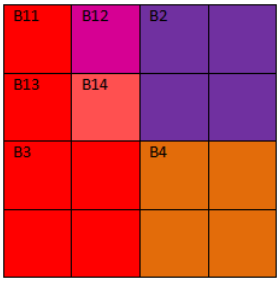

Figure 3: illustration of LEVEL 2 interpolation.

4.2 Directional interpolation

The deconvolution with the motion blur filter aims to create details of the image. The deconvolution can be formulated by the inverse problem $y = h \circledast x$ where h is the motion blur filter, y the observed image, x the unknown image and $\circledast$ is the convolution operator. The idea is to increase the size of the filter until the details are created but it is possible only with a well-designed y image built using the appropriate conditional interpolations. The motion filter owns two parameters, the distance L and the direction θ (or the angle of deconvolution) . Before the deconvolution we must increase the size of the image with a magnification factor γ to avoid the creation of blurred blocs on the image after the deconvolution. In the practice, γ depends of the geometry of the image (see Tables 2 and 3). The paramaters of conditional interpolations are known after a step of deep learning with a large database of HR and LR images and the better values are chosen to obtain the better interpolation, much less blurred than the other interpolation methods such as bicubic interpolations. The range of values for the parameter L begins from 0 to 19 and the range of values begins from 0 to 170 by step of 5 degrees. For an image, there is a resonance angle (by analogy with the resonance frequency) which appears when the user makes the motion deconvolution algorithm because the details are created only with this value of θ. We note $\hat{\theta}$ this unique value. The length parameter L depends of the size of the image, its value decreases when the size of the image is larger. This phenomenon leads us to build a new mathematical theory where the structure of images will be described with an angle of movement instead of a wavelet. The information can be represented as a matrix with different calls of LEVEL 1 interpolations. In the practice, we need only three or four LEVEL 1 interpolations, the first have the role of contrast enhancement and the two last correspond to the presmoothing. The smoothing has two components: the last call of LEVEL 1 interpolation just after the different areas are dissociated and the LEVEL 2 interpolation at the end of the interpolation process. We write the three parameters of the first LEVEL 1 occurrence $p2^{(1)}$, $p3^{(1)}$, $p4^{(1)}$. For the second occurrence $p2^{(2)}$, $p3^{(2)}$, $p4^{(2)}$, and for the third occurrence $p2^{(3)}$, $p3^{(3)}$, $p4^{(3)}$ (the fourth occurrence $p2^{(4)}$, $p3^{(4)}$, $p4^{(4)}$ is optional). There are three deconvolutions, the first $\gamma^{(1)}$, $L^{(1)}$, $\hat{\theta}^{(1)}$ is the more important to approach the right geometry, and the two others aim to

refine the result: $\gamma^{(2)}$, $L^{(2)}$, $\hat{\theta}^{(2)}$, $\gamma^{(3)}$, $L^{(3)}$, $\hat{\theta}^{(3)}$. Here $\gamma^{(1)}$=γ, $\theta^{\hat{(1)}}$=$\hat{\theta}$ (always) and $\gamma^{(2)}$=$\gamma^{(3)}$=1 in general.

$$\text{LABLANCHE}=\begin{pmatrix} p2^{(1)} & p3^{(1)} & p4^{(1)} \\ 255 & 255 & 255 \\ \gamma^{(1)} & L^{(1)} & \theta^{\hat{(1)}} \\ Source^{(1)} & Amount^{(1)} & Noise^{(1)} \\ p2^{(2)} & p3^{(2)} & p4^{(2)} \\ 255 & 255 & 255 \\ 1 & L^{(2)} & \theta^{\hat{(2)}} \\ Source^{(2)} & Amount^{(2)} & Noise^{(2)} \\ p2^{(3)} & p3^{(3)} & p4^{(3)} \\ 255 & 255 & 255 \\ 1 & L^{(3)} & \theta^{\hat{(3)}} \\ Source^{(3)} & Amount^{(3)} & Noise^{(3)} \\ p2^{(4)} & p3^{(4)} & p4^{(4)} \\ 255 & 255 & 255 \\ 255 & 255 & 255 \end{pmatrix} \quad (1)$$

Source is the source image (DVC: Digital Video Camera or OFC: Old Film Camera), *Amount* (to apply to the image) (100, 125, 150, 200, 250 or 300 %) and $Noise$ the choice Remove noise (Yes/No or DO: Dark Only or LO: Light Only).

We indicate the motion blur filter h for L=13 and θ=105° (13 columns and 5 rows matrix) which is optimal for Marie Bonneau (see Figure 4).

$$h=\begin{pmatrix} 0.0384 & 0.0310 & 0 & 0 & 0 \\ 0.0273 & 0.0507 & 0 & 0 & 0 \\ 0.0078 & 0.0703 & 0 & 0 & 0 \\ 0 & 0.0612 & 0.0169 & 0 & 0 \\ 0 & 0.0416 & 0.0364 & 0 & 0 \\ 0 & 0.0221 & 0.0560 & 0 & 0 \\ 0 & 0.0026 & 0.0755 & 0.0026 & 0 \\ 0 & 0 & 0.0560 & 0.0221 & 0 \\ 0 & 0 & 0.0364 & 0.0416 & 0 \\ 0 & 0 & 0.0169 & 0.0612 & 0 \\ 0 & 0 & 0 & 0.0703 & 0.0078 \\ 0 & 0 & 0 & 0.0507 & 0.0273 \\ 0 & 0 & 0 & 0.0310 & 0.0384 \end{pmatrix} \quad (2)$$

h is a vector for horizontal and vertical direction and a matrix otherwise. The filter h plays the role of the matrix Ψ in the parsimonious research (see Compressed Sensing section). The columns are symmetrical to the central column, but they are reversed.

L \ θ	5°	15°	25°	35°	45°	55°	65°	75°	85°	95°	105° ...
0	×	×	×	×	×	×	×	×	×	×	×
1	×	×	×	×	×	×	×	×	×	×	×
2	×	×	×	×	×	×	×	×	×	×	×
3	×	×	×	$(L^3, \hat{\theta}^3)$	×	×	×	×	×	×	×
4	×	×	×	×	×	×	×	×	×	×	×
5	$(L^2, \hat{\theta}^2)$	×	×	×	×	×	×	×	×	×	×
6	×	×	×	×	×	×	×	×	×	×	×
7	×	×	×	×	×	×	×	×	×	×	×
8	×	×	×	×	×	×	×	×	×	×	×
9	×	×	×	×	×	×	×	×	×	×	×
10	×	×	×	×	×	×	×	×	×	×	×
11	×	×	×	×	×	×	×	×	×	×	×
12	×	×	×	×	×	×	×	×	×	×	×
13	×	×	×	×	×	×	×	×	×	×	$(L^1, \hat{\theta}^1)$
14	×	×	×	×	×	×	×	×	×	×	×
15	×	×	×	×	×	×	×	×	×	×	×
16	×	×	×	×	×	×	×	×	×	×	×
17	×	×	×	×	×	×	×	×	×	×	×

Figure 4: motion deconvolution grid, $(L, \hat{\theta})$ is optimal for Marie Bonneau.

5.Experiments

In the case where step and q are not even numbers, for example for step=3, we define q=E(step/2) where E is the integer part. The B1 bloc is a 2 by 2 pixels bloc but the sizes of B2, B3 and B4 are different. The B2 bloc is a 2 by 1 pixels bloc, the B3 bloc is the 1 by 2 pixels bloc and B4 bloc is a pixel. The B2 bloc is stretched in the direction of the right adjacent bloc and the B3 bloc is stretched in the direction of the bottom adjacent bloc which enables to say that the geometry of this interpolation method is optimal for the case where step=3 (see Figure 5).

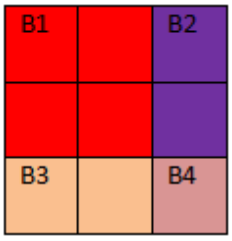

Figure 5: illustration of the case 3 by 3 pixels.

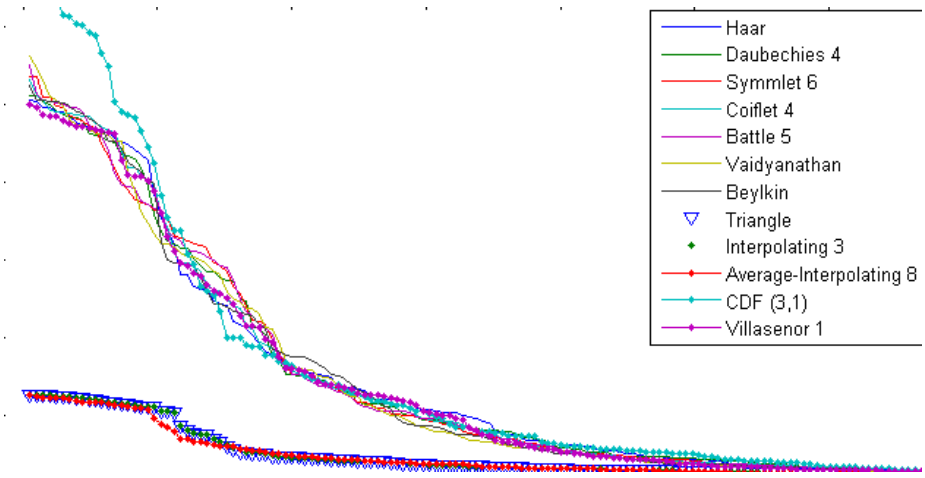

Figure 6: Comparison of the decreases of the different wavelet families coefficients in absolute value (Marie Bonneau image), the largest Villasenor coefficients (purple dot curve) are lower than for other wavelet families and their decay is faster (smallest L1 norm). The interpolation wavelets magnitudes (Triangle, Interpolating, Average-Interpolating) are much lower but are suitable only from 50% of randomly known pixels using L1-minimization (see Figure 10). The decay of CDF wavelet family is the fastest but the magnitude of larger CDF coefficients is higher than for the other wavelet families. We observed the same curves for all images.

The algorithm described before is the same with these new B2, B3 and B4 blocs and the L parameter is smaller because we need a weaker deconvolution than the deconvolution used in the case of 4 by 4 pixels. The angle of resonance $\hat{\theta}$ is the same for a given image. This case is important because it corresponds to 11 % of known pixels and we demonstrate that the 11 % larger coefficients approximation in the best wavelet base (in general Villasenor 1 or Villasenor 5) is very precise for a visual identification by the human eye (see the starry image on Figure 7). Unfortunately, this algorithm gives catastrophic results, so we can present only the case 4 by 4 pixels. We have an equivalence between the pixels ratio and the best wavelet larger coefficients keeped ratio in the quality of reconstruction and approximation. Villasenor 1 is the wavelet basis used in the JPEG 2000 standard. The best wavelets are Villasenor 1,2,3,4,5 (see Figure 6). The optimal wavelet for Marie Bonneau is Villasenor 5 (see Figures 7,8 and Table 1). The interest of our algorithm will be to obtain similar quality reconstructions from 8x8 low resolution images in comparison with 11% larger coefficients keeped approximations in the optimal wavelet basis (see Figures 9,10).

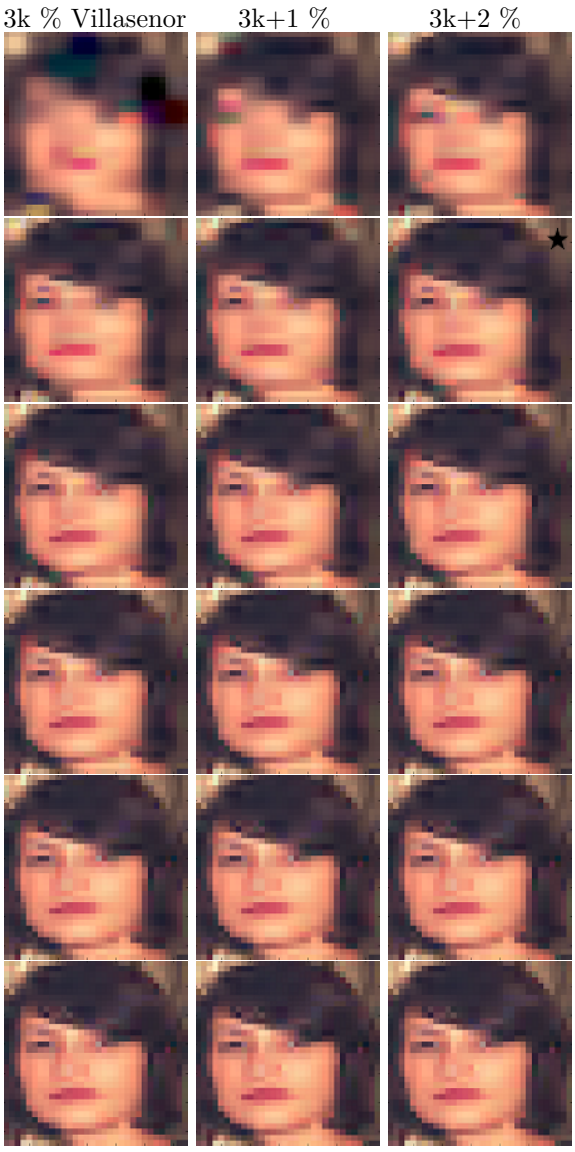

Figure 7: Approximation of Marie Bonneau with 6,7,8%(First line), 9,10,11% (Second line), 12,13,14%(Third line), 15,16,17%(Fourth line), 18,19,20%(Fifth line), 21,22,23%(Sixth line) of larger coefficients in Villasenor 5 wavelet basis.

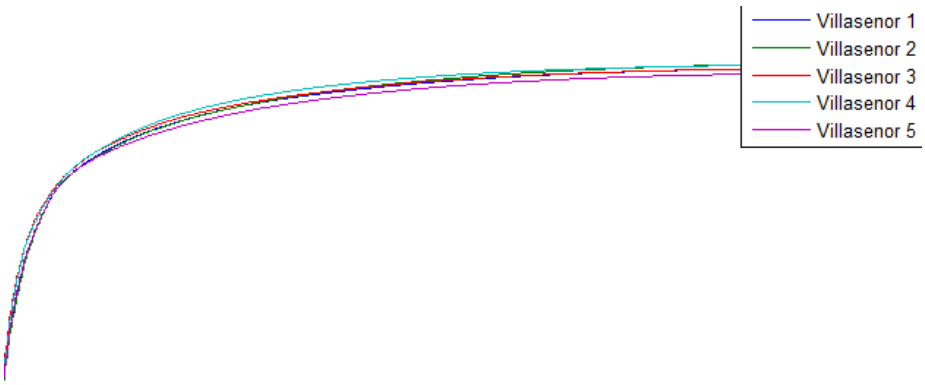

Figure 8: cumulative sums of the coefficients in absolute values of the Villasenor wavelets for Marie Bonneau (1) (illustrating technology image), the lower magnitude is the purple curve.

Table 1: table of test images.

Part	
Name 32x32	optimal wavelet
Google Brain (1)	Villasenor 1
Google Brain (2)	Villasenor 5
Google Brain (3)	Villasenor 1
Marie Bonneau (1)	Villasenor 5
Marie Bonneau (2)	Villasenor 1
Ellie Goulding	Villasenor 1
Ariana Grande	Villasenor 5
Shailene Woodley	Villasenor 5
Man	Villasenor 1
Eye	Villasenor 1
Meghan Markle	Villasenor 5

We use eleven test images of 32x32 pixels for our algorithm: Google Brain (3 images), Marie Bonneau (2 images), Ellie Goulding, Ariana Grande, Man, Shailene Woodley, Ronald Coifman (eye) and Meghan Markle. We give the optimal wavelet for each of the eleven test images (see Table 1) and the directional and conditional interpolations parameters obtained after tests on a large dataset of images with different geometries. We have chosen one of the best combination of parameters which brings out the resonance angle of motion deconvolution following the scheme described below (see Figure 9), the magnification factor γ is learned and known for each image (see Tables 2 and 3).

$i \leftarrow 1$;
$treshold \leftarrow value$;
Inputs: $\mathcal{I}$, $\mathcal{H}$, $treshold$
while $\|\mathcal{I} - \mathcal{H}\|_2^2 + \lambda\mathcal{R}(\mathcal{H}) \geq treshold$ **do**
  $\hat{\mathcal{H}} \leftarrow \underset{p2^{(i)},p3^{(i)},p4^{(i)},L^{(i)},\theta^{(i)},Source^{(i)},Amount^{(i)},Noise^{(i)}}{\arg\min} \|\mathcal{I} - \mathcal{H}\|_2^2 + \lambda\mathcal{R}(\mathcal{H})$;
  $p2^{(i)} \leftarrow \hat{p2^{(i)}}$;
  $p3^{(i)} \leftarrow \hat{p3^{(i)}}$;
  $p4^{(i)} \leftarrow \hat{p4^{(i)}}$;
  $L^{(i)} \leftarrow \hat{L^{(i)}}$;
  $\theta^{(i)} \leftarrow \hat{\theta^{(i)}}$;
  $Source^{(i)} \leftarrow \hat{Source^{(i)}}$;
  $Amount^{(i)} \leftarrow \hat{Amount^{(i)}}$;
  $Noise^{(i)} \leftarrow \hat{Noise^{(i)}}$;
  $i \leftarrow i + 1$;
  $\mathcal{H} \leftarrow \hat{\mathcal{H}}$;
end
$\hat{\mathcal{H}} \leftarrow \underset{p2^{(i)},p3^{(i)},p4^{(i)}}{\arg\min} \|\mathcal{I} - \mathcal{H}\|_2^2 + \lambda\mathcal{R}(\mathcal{H})$;
Output: $\hat{\mathcal{H}}$

$\mathcal{R}$ is a regulator and λ is the compromise between the norm minimization and the regularization, $\mathcal{I}$ is the original image, $\hat{\mathcal{H}}$ is the solution obtained with optimal parameters and $\mathcal{H}$ is the 8x8 low resolution input image. It is known to use total variation minimization, but here we define $\mathcal{R}$ as the inverse of the sum of 8x8 windows contrasts of the image because on the one hand the aim of these constraints is to enhance the contrast and on the other hand the contrast of pixels is low inside a 4x4 window but is very high in a 8x8 window (close to 1). For a 32x32 image, there are 16 windows of 8 by 8 pixels and $\mathcal{R}=\frac{1}{\sum_{i=1}^{16} C_i}$ where C_i is the contrast of the i^{th} bloc defined by $\frac{I_{max}-I_{min}}{I_{max}+I_{min}}$ (I_{max} and I_{min} are the maximum and the minimum intensity of the i^{th} bloc).

Table 2: table of results (interpolation).

Part		
Name 32x32	conditional interpolation parameters (Right image)	γ
Google Brain (1)	$p2^{(1)}$=63, $p3^{(1)}$=255, $p4^{(1)}$=20	3.80
Google Brain (2)	$p2^{(1)}$=65, $p3^{(1)}$=0, $p4^{(1)}$=65	3.40
Google Brain (3)	$p2^{(1)}$=195, $p3^{(1)}$=0, $p4^{(1)}$=0	3.62
Marie Bonneau (1)	$p2^{(1)}$=135, $p3^{(1)}$=10, $p4^{(1)}$=20	2.25
Marie Bonneau (2)	$p2^{(1)}$=88, $p3^{(1)}$=70, $p4^{(1)}$=0	2.25
Ellie Goulding	$p2^{(1)}$=85, $p3^{(1)}$=55, $p4^{(1)}$=0	2.20
Ariana Grande	$p2^{(1)}$=50, $p3^{(1)}$=225, $p4^{(1)}$=0	3.83
Shailene Woodley	$p2^{(1)}$=75, $p3^{(1)}$=0, $p4^{(1)}$=0	3.05
Man	$p2^{(1)}$=90, $p3^{(1)}$=98, $p4^{(1)}$=0	3.20
Eye	$p2^{(1)}$=105, $p3^{(1)}$=110, $p4^{(1)}$=0	2.05
Meghan Markle	$p2^{(1)}$=98, $p3^{(1)}$=60, $p4^{(1)}$=0	2.25

Table 3: table of results (deconvolution).

Part		
Name 32x32	deconvolution parameters (Right image)	γ
Google Brain (1)	L=16, θ=90°; L=7, θ=45°; L=15, θ=75°;	3.80
Google Brain (2)	L=15, θ=70°; L=6, θ=150°;	3.40
Google Brain (3)	L=17, θ=115°;	3.62
Marie Bonneau (1)	L=13, θ=105°; L=5, θ=5°; L=3, θ=35°;	2.25
Marie Bonneau (2)	L=12, θ=160°; L=11, θ=155°; L=2, θ=25°;	2.25
Ellie Goulding	L=11, θ=125°; L=9, θ=10°; L=5, θ=35°;	2.20
Ariana Grande	L=16, θ=100°; L=5, θ=160°; L=5, θ=60°; L=11, θ=35°; L=6, θ=180°;	3.83
Shailene Woodley	L=13, θ=120°; L=6, θ=20°;	3.05
Man	L=20, θ=140°; L=5, θ=120°; L=5, θ=5°;	3.20
Eye	L=10, θ=170°; L=5, θ=25°;	2.05
Meghan Markle	L=11, θ=105°;	2.25

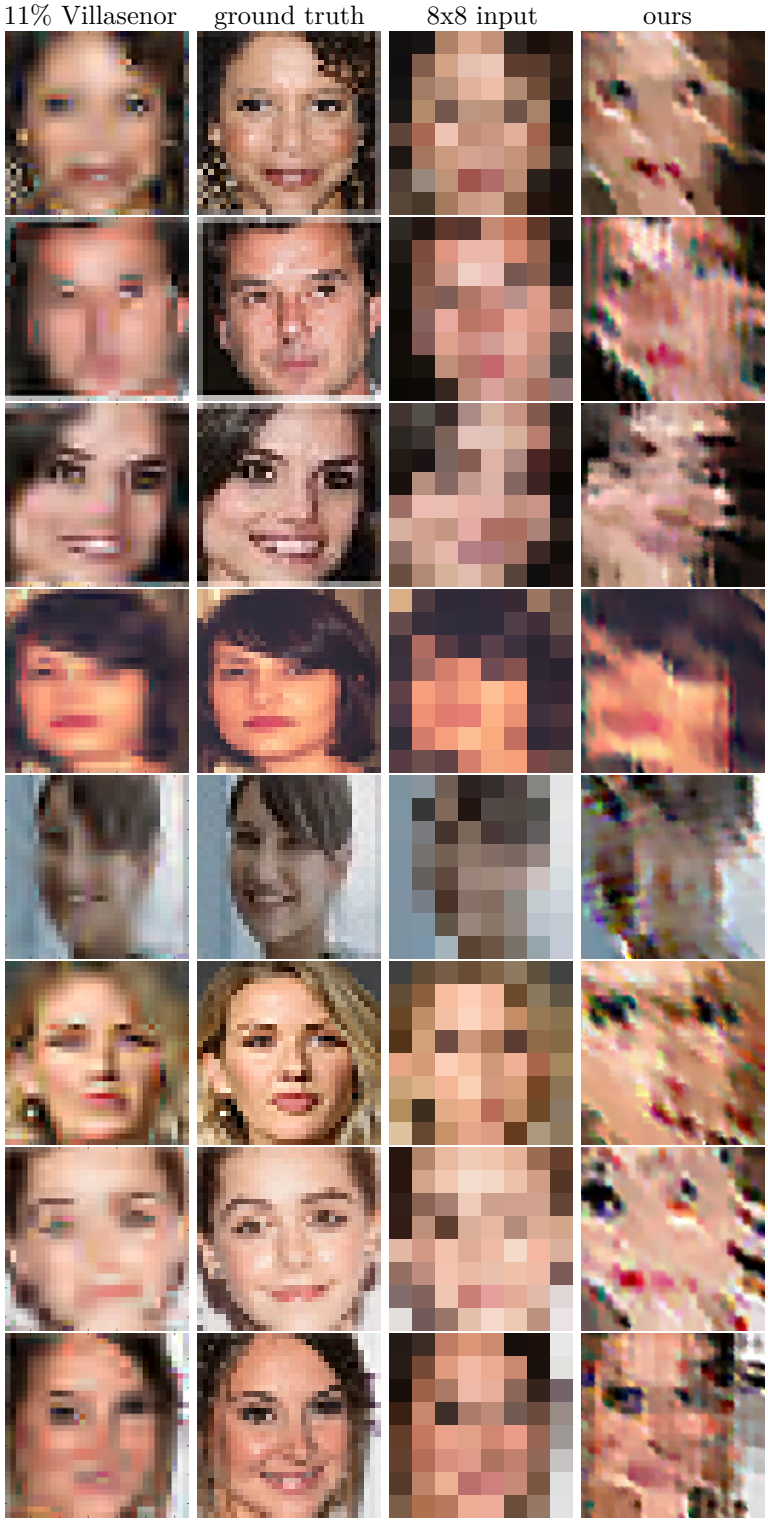
11% Villasenor
ground truth
8x8 input
ours

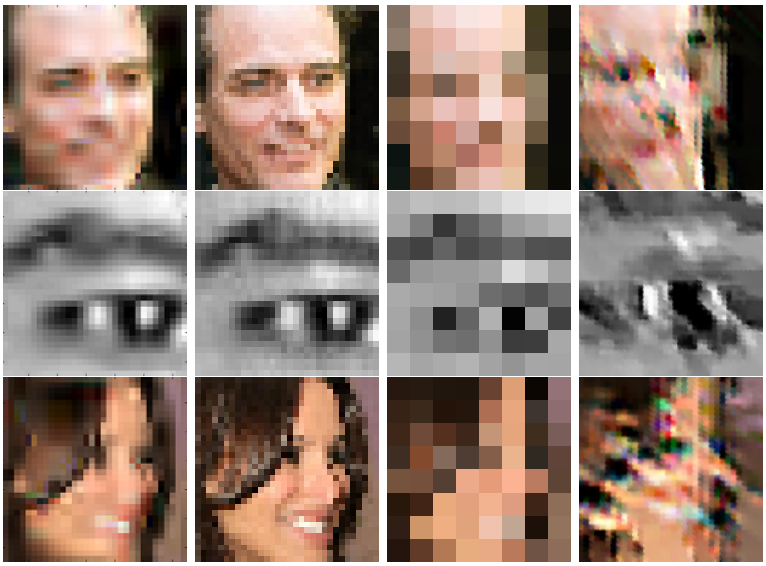

Figure 9: Reconstruction results (Right column) from 8x8 low resolution images (Middle Right column), 32x32 ground truth images (Middle Left column) and 11% of Villasenor 1/Villasenor 5 larger coefficients approximations (Left column).

We give the complete data results according to the model described before. The deconvolution algorithm is very easy to use and the choice of parameters is easy and fast for the user who can see the different possibilities for the reconstruction. Moreover the complexity of interpolations is very low because we use only three adjacent blocs (see below the Left matrix: Google Brain (1), the Middle matrix: Google Brain (2) and the Right matrix: Marie Bonneau (1)).

$$\begin{pmatrix} 63 & 255 & 20 \\ 255 & 255 & 255 \\ 3.80 & 16 & 90° \\ DVC & LO & 100\% \\ 1 & 7 & 45° \\ DVC & LO & 75\% \\ 1 & 15 & 75° \\ DVC & DO & 0\% \\ 65 & 0 & 65 \\ 255 & 255 & 255 \\ 255 & 255 & 255 \end{pmatrix} ; \begin{pmatrix} 65 & 0 & 65 \\ 255 & 255 & 255 \\ 3.40 & 15 & 70° \\ OFC & YES & 300\% \\ 65 & 0 & 65 \\ 255 & 255 & 255 \\ 1 & 6 & 150° \\ DVC & YES & 75\% \\ 75 & 0 & 0 \\ 255 & 255 & 255 \\ 1 & 6 & 155° \\ DVC & DO & 50\% \\ 75 & 0 & 0 \\ 255 & 255 & 255 \\ 255 & 255 & 255 \end{pmatrix} ; \begin{pmatrix} 135 & 10 & 20 \\ 255 & 255 & 255 \\ 2.25 & 13 & 105° \\ DVC & DO & 100\% \\ 1 & 5 & 5° \\ DVC & LO & 150\% \\ 1 & 3 & 35° \\ DVC & AUTO & 125\% \\ 135 & 10 & 20 \\ 255 & 255 & 255 \\ 255 & 255 & 255 \end{pmatrix} ; \left(\ (1), (2), (3) \ \right)$$

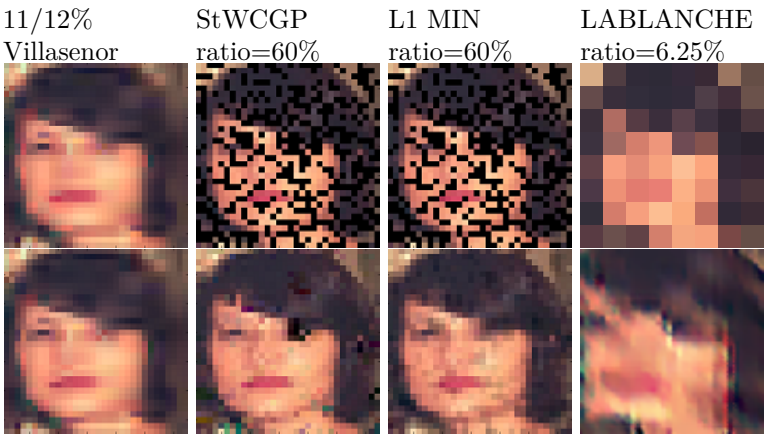

Figure 10: Comparison of the different reconstruction methods. From Left to Right: 11% and 12% of Villasenor 5 larger coefficients approximations (Left column), Stagewise Weak Conjugate Gradient Pursuit (StWCGP) in Villasenor 5 basis from 60% of randomly known pixels (Middle Left column), L1-Minimization in Average-Interpolating 8 basis from 60% of randomly known pixels (Middle Right column) and our method (Right column) from 6.25% of known pixels (8x8 low resolution input). Our method gives similar quality results than Compressed Sensing from 60% of pixels, but with only 6.25% of pixels. Moreover, it is easier to sample the image with a regular grid at the industrial level, therefore our algorithm can represent a new possible technological solution.

6.Conclusion

We have introduced a new class of algorithms based on new interpretations of deconvolution. The motion deconvolution is used to reconstruct details of the image instead of deblur forensic images. We note that the complexity is low and this process is easy to compute in comparison with deep learning, compressed sensing, mixture of both or categorization of zones. In the future, it would be interesting to find a better deconvolution algorithm and to find a trick to understand the links between conditional interpolations and the optimal angle of the deconvolution. The interpretation of these results is to see images as a combination of angles generated by conditional interpolations and the coherence of these angles is achieved with the optimal orientation of the motion deconvolution.

Acknowledgments

We thank to Jean Marc Azais (Institut de Mathématiques de Toulouse) and mostly Charles Dossal because his help has been very precious in our work to compute biorthogonal wavelet bases for large scale problems inside StWCGP algorithm (inversion of the analysis and synthesis wavelet filters for the calculation

of the multiplication by the transposed matrix), without his help me and my father couldn't have identified the transfer between the parsimonious research (L1-Minimization and L0-Minimization) and the decoherent research (conditional interpolations) when the information pixels rate decreases.
Of course, I would like to thank my father Gérard LABLANCHE and my mother Marie-Thérèse LABLANCHE.
Finally, I thank to OYAGAA AYOO YISSAA to give me courage to pursue my research work (see `https://www.ummo-sciences.org/fr/W2.htm`). *"Est ce une image de OEOE 95 dans l'image d'en-tête de compte OOMO TOA ? Oui. Son visage a été pixélisé d'un portrait afin de masquer les détails. Cependant il est clairement reconnaissable"*.

References

[1] Yonina C.Eldar and Gitta Kutyniok. *Compressed Sensing Theory and Applications*. Cambridge, 2012.

[2] Stephane Mallat. *Une exploration des signaux en ondelettes*. les editions de l'ecole polytechnique, 2000.

[3] Charles Dossal *Estimation de fonctions geometriques et deconvolution, These pour l'obtention du titre de Docteur de L'Ecole Polytechnique,* le 5 Decembre 2005.

[4] Richard E.Blahut, Willard Miller, Jr, Calvin H.Wilcox, *Radar and Sonar Part I,* Springer-Verlag.

[5] Sung Cheol Park, Min Kyn Park and Moon Gi Kang, *Super-Resolution Image Reconstruction: A Technical Overview*, *IEEE SIGNAL PROCESSING MAGAZINE*, 1053-5888/03, May 2003.

[6] Pradeep Sen and Soheil Darabi, *Compressive Image Super-Resolution, Advanced Graphics Lab*, *Department of Electrical and Computer Engineering, University of New Mexico, USA, New Mexico*, 1235-1242, 2009 IEEE.

[7] Jianchao Yang, John Wright, Thomas S.Huang, Yi Ma, *Image SuperResolution via Sparse Representation, IEEE Transactions on image processing*, vol.19, pp. 2861-2873, November 2010.

[8] Michael Elad and Michal Aharon, *Image Denoising via Sparse and Redundant Representations over Learned Dictionaries*, *IEEE Transactions on image processing*, vol.15, pp. 3736-3745, December 2006.

[9] Michal Irani, Shmuel Releg, *Image Sequence Enhancement using multiple motions analysis*, *Institute of computer Science, The Hebrew University of Jerusalem*, 0-8186-2855-3/92, 1992 IEEE.

[10] John Wright, Allen Y. Yang, Arvind Ganesh, S.Shankar Sastry, Yi Ma, *Robust Face Recognition via Sparse Representation*, *Transactions on pattern Analysis and Machine Intelligence*, vol.31, pp.210-227, February 2009 IEEE.

[11] Hong Chang, Dit-Yan Yeung, Yiming Xiong, *Super-Resolution Through Neighbor Embedding, Hong-Kong University of Science and Technology, Computer Society Conference on Computer Vision and Pattern Recognition*, 2004 IEEE.

Sébastien LABLANCHE received the master degree in statistics at Université Paul Sabatier Toulouse III in 2012, the master's degree in signal processing and the bachelor's degree in pure mathematics at Université Bordeaux 1 in 2010 and 2008. The patent n° FR 1855485 is the intellectual property of him. His research interests are image processing and information theory. He lead this work with the background of Université Paul Sabatier.

Gérard LABLANCHE received the bachelor's degree in information technology at Conservatoire National des Arts et Métiers in 1967. His research interests are automatic calculation and scientific computing. He is an expert in object-oriented programming and information processing algorithms, and he is the author of the source code which enables to realize interpolation experiments in an optimal manner.